

*Developing methods for identifying the inflection
point of a convex/concave curve*

Demetris T. Christopoulos^{1,2}

¹National and Kapodistrian University of Athens, Department of Economics

²dchristop@econ.uoa.gr, dem.christop@gmail.com

August 5, 2014

Abstract

We are introducing two methods for revealing the true inflection point of data that contains or not error. The starting point is a set of geometrical properties that follow the existence of an inflection point p for a smooth function. These properties connect the concept of convexity/concavity before and after p respectively with three chords defined properly. Finally a set of experiments is presented for the class of sigmoid curves and for the third order polynomials.

MSC2000. Primary 65H99, Secondary 62F12

Keywords. inflection point estimation, convex/concave curve, sigmoid curve, third order polynomial, ESE, EDE

1 Introducing geometrical methods

The finding of the inflection point is performed by adopting a suitable model and then with regression or maximum likelihood estimation techniques. Another approach is that of the Differential Geometry view, when we define a proper measure of discrete curvature and then we choose the points with such a measure as close to zero can be, see for example [12], [11] or Gaussian smoothing techniques, see [14]. A review of the relevant shape analysis methods can be found in [13].

We are going to present two new methods for identifying the inflection point of any given convex/concave curve based on the definition and its geometrical properties only and without any regression or splines representation. We will use a *generalization of bisection method in root finding* by choosing two points where the inflection point is between and then by taking the middle point as an estimator. The methods that will be presented will be able to iteratively converge to the actual inflection point in a manner similar to that of bisection method. Before starting it is necessary to give some preliminary definitions.

1.1 Preliminary Definitions

Let a function $f : [a, b] \rightarrow R$, $f \in C^{(n)}$, $n \geq 2$ which is convex for $x \in [a, p]$ and concave for $x \in [p, b]$, p is the unique inflection point of f in $[a, b]$ and let an arbitrary $x \in [a, b]$.

Definition 1.1 *Total, left and right chord are the lines connecting points $\{(a, f(a)), (b, f(b))\}$, $\{(a, f(a)), (x, f(x))\}$ and $\{(x, f(x)), (b, f(b))\}$ with Cartesian equations $g(x)$, $l(x)$ and $r(x)$ respectively.*

If $cx + dy + e = 0$ is the equation of the total chord, then by using elementary Analytical Geometry methods we can prove that the coefficients are

$$c = \frac{f(b)-f(a)}{b-a} \quad d = -1 \quad e = \frac{bf(a)-af(b)}{b-a} \quad (1)$$

Definition 1.2 *Distance from total, left and right chord are the functions $F, F_l, F_r : [a, b] \rightarrow R$ with:*

$$F(x) = f(x) - g(x) \quad (2)$$

$$F_l(x) = f(x) - l(x) \quad (3)$$

$$F_r(x) = f(x) - r(x) \quad (4)$$

So, recalling 1, the distance from total chord is equal to

$$F(x) = f(x) - \frac{(f(b) - f(a))x}{b-a} - \frac{bf(a) - af(b)}{b-a} \quad (5)$$

Definition 1.3 The *s-left* ($s_l(a, x)$) and *s-right* ($s_r(b, x)$) are the algebraic surfaces:

$$s_l(a, x) = \int_a^x F_l(t) dt \quad (6)$$

$$s_r(b, x) = \int_x^b F_r(t) dt \quad (7)$$

Definition 1.4 The *x-left* (x_l) and *x-right* (x_r) are values such that:

$$x_l = \underset{x \in [a, b + \delta_1]}{\operatorname{argmin}} \{s_l(a, x)\} \quad (8)$$

$$x_r = \underset{x \in [a - \delta_2, b]}{\operatorname{argmax}} \{s_r(b, x)\} \quad (9)$$

with $\delta_1, \delta_2 > 0$ taken as small as necessary for x_l, x_r to be unique unconstrained extremes in the corresponding intervals.

A graphical illustration of the above defined left and right-terms is presented at Figure 1 where we observe that when $x = x_l, x = x_r$ then we achieve the algebraic minimum $s_l(a, x)$ and maximum $s_r(b, x)$, respectively. The motivation for the *left-* and *right-* naming was due to the origin of the chords: left chord starts from the left edge while right chord starts from the right edge of the graph.

Definition 1.5 Normal algebraic distance of the curve point $(x, f(x))$ from the total chord 1.1 & 1 is the function $N : [a, b] \rightarrow R$ with:

$$N(x) = -\frac{cx + df(x) + e}{\sqrt{c^2 + d^2}} \quad (10)$$

For a convex/concave curve the above definition gives $N(x) < 0$ when $x < p$ and $N(x) > 0$ if $x > p$. Additionally, for computation purposes, by using 1, the above distance is

$$N(x) = -\frac{(f(b) - f(a))x - (b - a)f(x) + bf(a) - af(b)}{\sqrt{(f(b) - f(a))^2 + (b - a)^2}} \quad (11)$$

We call *standard partition (SP)* the strictly sorted grid of points, not necessary equal spaced:

$$\{x_i, i = 0, 1, \dots, n, a = x_0 < x_1 < \dots < x_n = b\} \quad (12)$$

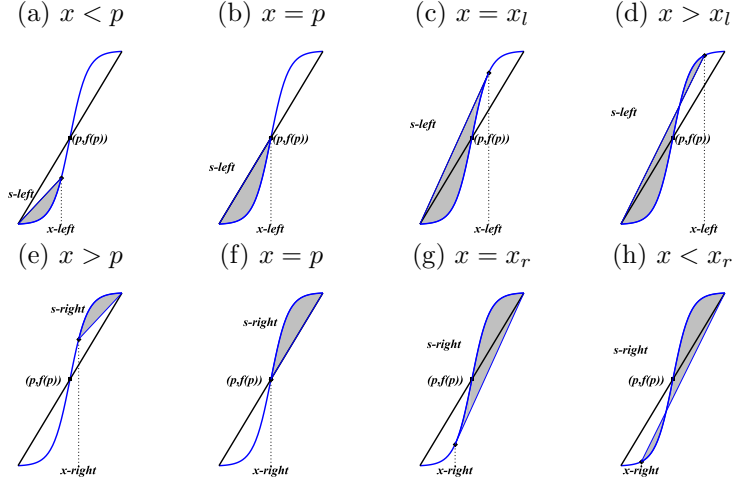


Figure 1: (color online) Illustration of the algebraic surfaces $s_l(a, x) < 0$ (a-d), $s_r(b, x) > 0$ (e-h) and of their corresponding points x_l, x_r .

The corresponding (x_i, f_i) data produced from f by the no error process:

$$\{f_i = f(x_i), i = 0, 1, \dots, n\} \quad (13)$$

If errors occur then we have the (x_i, ϕ_i) noisy data produced from f by the process:

$$\{\phi_i = f(x_i) + \epsilon_i, \epsilon_i \sim iid(0, \sigma^2) \ i = 0, 1, \dots, n\} \quad (14)$$

Our analysis is focused on uniform distributions ($\epsilon_i \sim U(-r, r)$) but it is applicable for every distribution with zero mean, for example the normal $N(0, \sigma^2)$. If the error distribution is not a zero mean one, then the results are ambiguous.

Definition 1.6 For the noisy data 14 we define the discrete distances from total, left and right chord as the values

$$\Phi(x_i) = \phi(x_i) - g(x_i), \ i = 0, 1, \dots, n \quad (15)$$

$$\Phi_l(x_i) = \phi(x_i) - l(x_i), \ i = 0, 1, \dots, n \quad (16)$$

$$\Phi_r(x_i) = \phi(x_i) - r(x_i), \ i = 0, 1, \dots, n \quad (17)$$

Definition 1.7 Function f is called symmetric around inflection point or symmetry around inflection point exists when:

$$f(p+x) - f(p) = f(p) - f(p-x), \forall x \in R \quad (18)$$

or

$$f(p+x) + f(p-x) - 2f(p) = 0, \forall x \in R \quad (19)$$

Definition 1.8 Function f is called locally (ϵ, δ) asymptotically symmetric around inflection point or local $\epsilon - \delta$ asymptotic symmetry exists when:

$$|f(p+x) + f(p-x) - 2f(p)| < \epsilon, \forall x \in (p-\delta, p+\delta) \quad (20)$$

Definition 1.9 For a function $f : [a, b] \rightarrow R$ we have that:

1. Data symmetry w.r.t. inflection point exists if $p - b = a - p$
2. Data left asymmetry w.r.t. inflection point exists if $p - b < a - p$
3. Data right asymmetry w.r.t. inflection point exists if $p - b > a - p$

Definition 1.10 A function $f : [a, b] \rightarrow R$ is called totally symmetric or total symmetry exist, if it is symmetric around inflection point p and also exist data symmetry w.r.t. p .

Definition 1.11 For every subsequent $x_i < x_j$ the elementary trapezoidal estimation holds:

$$\int_{x_i}^{x_j} f(x)dx \approx T_{i,j}(f, x_i, x_j) = \frac{f(x_i) + f(x_j)}{2}(x_j - x_i) \quad (21)$$

And for every standard partition the total trapezoidal estimation holds:

$$\int_a^b f(x)dx \approx T_{n+1}(f, a, b) = \sum_{i=0}^{n-1} T_{i,i+1}(f, x_i, x_{i+1}) \quad (22)$$

1.2 The Extremum Surface Method

We can prove that:

Lemma 1.1 The x -left (x_l) and x -right (x_r) are the points where left and right chord respectively are tangent to the graph $G(f)$.

Proof

1. Let $x_l \leq p$ be the first point where $l(x)$ cuts $G(f)$ from left to right. The function is convex for $x \in [a, p]$, so $G(f)$ is always below the left chord, thus giving a negative value for $s_l(a, x_l)$, which is increasing in absolute value as x_l departures from a to the right until point p . After inflection point f is increasing, so it is possible to continue adding negative values of surface until the point $x^* \in (p, b]$ for which $G(f)$ and $l(x)$ have one only common point.

If we continue beyond this point, then $G(f)$ and $l(x)$ have again two common points (x_1, y_1) ,

(x_2, y_2) , $x_1 < x_2$ such that $s_l(a, x_1) < 0$ and $s_l(x_1, x_2) > 0$, thus we have started adding positive values to the $s_l(a, x)$ and this leads to a raise of the total value $s_l(a, x) = s_l(a, x_1) + s_l(x_1, x_2)$.

So, function $s_l(a, x)$ is decreasing for $x \in [a, x^*]$ and increasing for $x \in [x^*, b]$, thus $x^* > p$ is a local minimum and we call it x_l .

2. Let $x_r \geq p$ be the first point where $r(x)$ cuts $G(f)$ from right to left. The function is concave for $x \in [p, b]$, so $G(f)$ is always above the right chord, thus giving a positive value for $s_r(b, x_r)$, which is increasing as x_r departures from b to the left until inflection point p . After that point f is still above the right chord until the point $x^* \in [a, p]$ for which $G(f)$ and $r(x)$ have only one common point.

If we continue again beyond this point, then $G(f)$ and $r(x)$ have again two common points $(x_1, y_1), (x_2, y_2)$, $x_1 > x_2$ such that $s_r(b, x_1) > 0$ and $s_r(x_1, x_2) < 0$, so we have started adding negative values to the $s_r(b, x)$ and this leads to a reduction of the total value $s_r(b, x) = s_r(b, x_1) + s_r(x_1, x_2)$.

So, function $s_r(b, x)$ is increasing for $x \in [a, x^*]$ and decreasing for $x \in [x^*, b]$, thus $x^* < p$ is a local minimum and we call it x_r .

□

Corollary 1.1 *For the definitions of 1.4 it holds*

$$x_l = \arg_{x \in [a, b + \delta_1]} \left\{ f'(x) = \frac{f(x) - f(a)}{x - a} \right\} \quad (23)$$

$$x_r = \arg_{x \in [a - \delta_2, b]} \left\{ f'(x) = \frac{f(b) - f(x)}{b - x} \right\} \quad (24)$$

with $\delta_1, \delta_2 > 0$ taken as small as necessary for x_l, x_r to be unique unconstrained solutions in the corresponding intervals.

This tangency condition is obvious from Figure 1c.

Corollary 1.2 *Let a function $f : [a, b] \rightarrow \mathbb{R}$, $f \in C^{(n)}$, $n \geq 2$ which is convex for $x \in [a, p]$ and concave for $x \in [p, b]$. Then we have one of the following possibilities:*

1. If $x_l, x_r \in [a, b]$ then $a \leq x_r < x_l \leq b$
2. If $x_l \notin [a, b]$ then $x_l > b$
3. If $x_r \notin [a, b]$ then $x_r < a$

We define the next theoretical estimator of the inflection point:

Definition 1.12 *The theoretical extremum surface estimator (TESE) is*

$$x_S = \begin{cases} \frac{x_l+x_r}{2} & , \quad x_l, x_r \in [a, b] \\ \frac{b+x_r}{2} & , \quad x_l > b \\ \frac{x_l+a}{2} & , \quad x_r < a \end{cases} \quad (25)$$

Lemma 1.2 *If the mesh $\lambda(n)$ of the standard partition is such that:*

$$\lim_{n \rightarrow \infty} n\lambda(n)^2 = 0$$

then $T_{n+1}(\phi, a, b)$ is a consistent estimator of the true value of $T_{n+1}(f, a, b)$.

Proof

For every subsequent $x_i < x_{i+1}$ the elementary trapezoidal estimation is:

$$T_{i,i+1}(\phi, x_i, x_{i+1}) = \frac{x_{i+1} - x_i}{2} \phi(x_i) + \frac{x_{i+1} - x_i}{2} \phi(x_{i+1}) \quad (26)$$

Taking the expected value we obtain:

$$\begin{aligned} E(T_{i,i+1}(\phi, x_i, x_{i+1})) &= \frac{x_{i+1} - x_i}{2} E(\phi(x_i)) + \frac{x_{i+1} - x_i}{2} E(\phi(x_{i+1})) \\ &= \frac{x_{i+1} - x_i}{2} f(x_i) + \frac{x_{i+1} - x_i}{2} f(x_{i+1}) \\ &= T_{i,i+1}(f, x_i, x_{i+1}) \end{aligned} \quad (27)$$

so from the linearity of expected value we have also that:

$$E(T_{n+1}(\phi, a, b)) = \sum_{i=0}^{n-1} E(T_{i,i+1}(\phi, x_i, x_{i+1})) = T_{n+1}(f, a, b) \quad (28)$$

Thus our estimator is unbiased.

We continue by computing the variance of the elementary trapezoidal estimation:

$$\begin{aligned}
V(T_{i,i+1}(\phi, x_i, x_{i+1})) &= \left(\frac{x_{i+1}-x_i}{2}\right)^2 V(\phi(x_i)) + \left(\frac{x_{i+1}-x_i}{2}\right)^2 V(\phi(x_{i+1})) \\
&= \frac{(x_{i+1}-x_i)^2}{4} \sigma^2 + \frac{(x_{i+1}-x_i)^2}{4} \sigma^2 \\
&= \frac{(x_{i+1}-x_i)^2}{2} \sigma^2
\end{aligned} \tag{29}$$

We have two cases.

If standard partition is equal spaced, then $x_{i+1} - x_i = \frac{b-a}{n}$ and we obtain:

$$V(T_{i,i+1}(\phi, x_i, x_{i+1})) = \frac{(b-a)^2}{2n^2} \sigma^2 \tag{30}$$

Let's compute now the variance of estimator $T_{n+1}(\phi, a, b)$:

$$\begin{aligned}
V(T_{n+1}(\phi, a, b)) &= V\left(\sum_{i=0}^{n-1} T_{i,i+1}(\phi, x_i, x_{i+1})\right) \\
&= n V(T_{i,i+1}(\phi, x_i, x_{i+1})) \\
&= n \frac{(b-a)^2}{2n^2} \sigma^2 \\
&= \frac{(b-a)^2}{2n} \sigma^2
\end{aligned} \tag{31}$$

so clearly it holds:

$$\lim_{n \rightarrow \infty} V(T_{n+1}(\phi, a, b)) = \lim_{n \rightarrow \infty} \frac{(b-a)^2}{2n} \sigma^2 = 0$$

For the second case, if standard partition is not equal spaced then the mesh or norm of the partition is

$$\lambda(n) = \max_{i=0, \dots, n-1} (x_{i+1} - x_i)$$

Then it is easy to show that:

$$V(T_{i,i+1}(\phi, x_i, x_{i+1})) \leq \frac{\lambda(n)^2}{2} \sigma^2 \tag{32}$$

and the total variance is:

$$V(T_{n+1}(\phi, a, b)) \leq \frac{\sigma^2}{2} n \lambda(n)^2 \xrightarrow{n \rightarrow \infty} 0 \tag{33}$$

from our hypothesis. So the estimator is consistent. \square

Now we are able to compute using our trapezoidal rule 1.11 data estimations for $s_l(x_0, x_j)$ and $s_r(x_n, x_j)$:

Definition 1.13 *The data estimators of the algebraic surfaces of 1.3 are*

$$s_{l,j+1}(x_0, x_j) = T_{j+1}(\Phi_l, x_0, x_j) \quad (34)$$

$$s_{r,n-j+1}(x_n, x_j) = T_{n-j+1}(\Phi_r, x_j, x_n) \quad (35)$$

$$(36)$$

It is time to define the next data estimators for x_l, x_r .

Definition 1.14 *The χ_l, χ_r are values such that:*

$$\chi_l = x_{j_l} \quad (37)$$

$$j_l = \underset{j \in [1, n]}{\operatorname{argmin}} \{s_{l,j+1}(x_0, x_j)\}$$

$$\chi_r = x_{j_r} \quad (38)$$

$$j_r = \underset{j \in [0, n-1]}{\operatorname{argmax}} \{s_{r,n-j+1}(x_n, x_j)\}$$

$$(39)$$

We define now the noisy data estimator of the inflection point:

Definition 1.15 *The data extremum surface estimator (ESE) is*

$$\chi_S = \frac{\chi_l + \chi_r}{2} \quad (40)$$

Lemma 1.3 *The ESE is a consistent estimator of TESE with all relevant integrals calculated via trapezoidal rule.*

Proof

We have proven in Lemma 1.2 that trapezoidal rule for the noisy data gives a consistent estimator for the trapezoidal estimation of the actual data, thus χ_l, χ_r are consistent estimators of the true x_l, x_r respectively, with relevant integrals trapezoidal calculated.

If the interval $[a, b]$ is such that both $x_l, x_r \in [a, b]$ then ESE is a consistent estimator of trapezoidal calculated $x_S = \frac{x_l + x_r}{2}$.

If $x_l > b$ then recalling Proof of Lemma 1.1 $s_l(a, x)$ is a decreasing function, so the minimum χ_l is achieved when $\chi_l = b$, the rightmost value of $[a, b]$.

If $x_r < a$ then recalling Proof of Lemma 1.1 $s_r(b, x)$ is an increasing function, so the maximum χ_r is achieved when $\chi_r = a$, the leftmost value of $[a, b]$.

So, for every possible case, ESE is a consistent estimator of the TESE given by integrals calculated via trapezoidal rule. \square

We have to make a remark about the concept of convex or concave area, as is

defined in [12] and as defined in this work. There the concept of area that is computed is a summation of the distances from a chord and curve, between two critical points, while our approach computes an actual geometrical area by using the trapezoidal rule.

1.3 The Extremum Distance Method

Definition 1.16 *The x_F -left (x_{F1}), x_F -right (x_{F2}) and x_N -left (x_{N1}), x_N -right (x_{N2}) are values such that:*

$$x_{F1} = \underset{x \in [a-\delta_1, b]}{\operatorname{argmin}} F(x), \quad x_{F2} = \underset{x \in [a, b+\delta_2]}{\operatorname{argmax}} F(x) \quad (41)$$

$$x_{N1} = \underset{x \in [a-\delta_1, b]}{\operatorname{argmin}} N(x), \quad x_{N2} = \underset{x \in [a, b+\delta_2]}{\operatorname{argmax}} N(x) \quad (42)$$

with $\delta_1, \delta_2 > 0$ taken as small as necessary for x_{F1}, x_{F2} to be unique unconstrained extremums in the corresponding intervals.

The defined points and the corresponding line segments can be found at the Figure 2 where it is also obviously shown that when we achieve a stationary value for $F(x)$ of 1.2, then we achieve also the relevant stationary value for normal distance $N(x)$ of 1.5, since the vector defined from $N(x)$ is just the orthogonal projection of the vector defined from $F(x)$ at the normal vector to the total chord. Now we shall prove the next useful Lemma.

Lemma 1.4 *For the definitions of 1.16 it holds*

$$x_{F1,2} = \underset{x \in [a-\delta_1, b+\delta_2]}{\operatorname{arg}} \left\{ f'(x) = \frac{f(b) - f(a)}{b - a} \right\} \quad (43)$$

with $\delta_1, \delta_2 > 0$ taken as small as necessary for x_{F1}, x_{F2} to be unique unconstrained extremes in the corresponding intervals.

Proof

We have extended the interval $[a, b]$ such that there exist (both unconstrained) a local minimum and a local maximum inside. For our convex/concave case let $\rho \in [a-\delta_1, b+\delta_2], \rho \notin \{a, b\}$ is the internal root of $F(x)$. Then we have that $F(x) < 0, x \in [a-\delta_1, \rho]$ and $F(x) > 0, x \in [\rho, b+\delta_2]$, because function is convex near a and concave near b. Thus the local minimum exists at $[a-\delta_1, \rho]$ and the local maximum lies in $[\rho, b+\delta_2]$. If we take the first derivative we have that:

$$F'(x) = f'(x) - g'(x) = f'(x) - \lambda = 0 \Rightarrow f'(x) = \lambda \quad (44)$$

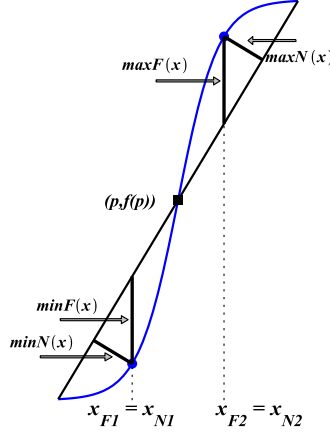


Figure 2: (color online) Illustration of points x_{F1} , x_{F2} and the corresponding distances $\min F(x)$, $\max F(x)$

where $\lambda = \frac{f(b)-f(a)}{b-a}$ is the slope of the total chord. But the above equation must hold for both local minimum/maximum $x_{F1,2}$, so it is necessary to hold:

$$f'(x_{F1}) = f'(x_{F2}) = \frac{f(b) - f(a)}{b - a} \quad (45)$$

We can also check the second derivative which is:

$$F''(x) = f''(x) \quad (46)$$

so it holds $F''(x_{F1}) = f''(x_{F1}) > 0$ and $F''(x_{F2}) = f''(x_{F2}) < 0$, i.e. we have the correct signs for local minimum and maximum respectively. \square

Corollary 1.3 *Let a function $f : [a, b] \rightarrow \mathbb{R}$, $f \in C^{(n)}$, $n \geq 2$ which is convex for $x \in [a, p]$ and concave for $x \in [p, b]$. Then we have one of the following possibilities:*

1. If $x_{F1}, x_{F2} \in [a, b]$ then $a \leq x_{F1} < x_{F2} \leq b$
2. If $x_{F1} \notin [a, b]$ then $x_{F1} < a$
3. If $x_{F2} \notin [a, b]$ then $x_{F2} > b$

We define the next theoretical estimator of the inflection point:

Definition 1.17 *The theoretical extremum distance from total chord estimator (TEDE) is such that*

$$x_D = \frac{x_{F1} + x_{F2}}{2} \quad (47)$$

Now we can define the data estimators of x_{F1}, x_{F2} and x_D .

Definition 1.18 *The data estimations of the points defined at 1.16 are*

$$\chi_{F1} = x_{j_1} \quad (48)$$

$$j_1 = \underset{j \in [0, n]}{\operatorname{argmin}} \{\Phi(x_j)\}$$

$$\chi_{F2} = x_{j_2} \quad (49)$$

$$j_2 = \underset{j \in [0, n]}{\operatorname{argmax}} \{\Phi(x_j)\}$$

Definition 1.19 *The extremum distance from total chord estimator (EDE) is*

$$\chi_D = \frac{\chi_{F1} + \chi_{F2}}{2} \text{ iff } \chi_{F2} \geq \chi_{F1} \quad (50)$$

Lemma 1.5 *The EDE is an unbiased estimator of TEDE.*

Proof

For all $\Phi(x_j), j = 0, 1, \dots, n$ it holds:

$$E(\Phi(x_j)) = F(x_j) \quad (51)$$

so if we take the noisy data instead of the true data it has to be also that:

$$E\left(\min_{j \in [0, n]} \{\Phi(x_j)\}\right) = \min_{j \in [0, n]} \{F(x_j)\} \quad (52)$$

$$E\left(\max_{j \in [0, n]} \{\Phi(x_j)\}\right) = \max_{j \in [0, n]} \{F(x_j)\}$$

□

At this stage we have to mention that there exists a similar work with distances from the chord, see [11], where a summation of the relevant distances from the chord is taken in order to define the concept of a *discrete curvature* for a planar curve.

Similar approach is that of [12], where it is also used a proper summation of the distances between the chord and the curve points. Here we do not define and we do not compute any kind of curvature, but we just choose only the two extreme distances needed for Definition 1.16.

1.4 Iterative application of geometrical methods

Another very important opportunity is the possibility of iterations like the well known *bisection method* in root finding. Recall that for a continuous function if $f(\alpha)f(\beta) < 0$ then exist $\xi \in (\alpha, \beta)$ such that $f(\xi) = 0$. Our ESE method always gives an interval that contains the true inflection point p or a point close to the edge a or b , if data is just convex (or just concave) and inflection point does not exist. EDE method also gives an interval in most cases, although it is more sensitive to errors, so it does not always give a point close to a or b , if simple convexity or concavity exist.

1. *ESE iterative method or Bisection-ESE or BESE*

We apply to initial data $\{(x_i, \phi_i), i = 0, \dots, n\}$ the ESE method and have the 0^{th} output for it:

$$[j_r^{(0)}, j_l^{(0)}], \chi_r^{(0)} = x_{j_r^{(0)}}, \chi_l^{(0)} = x_{j_l^{(0)}}, \chi_S^{(0)} = \frac{\chi_r^{(0)} + \chi_l^{(0)}}{2}$$

If and only if $j_l^{(0)} > j_r^{(0)}$, then we apply again ESE for data:

$$\{(x_i, \phi_i), i = j_r^{(0)}, \dots, j_l^{(0)}\}$$

and obtain the 1^{st} output for it:

$$[j_r^{(1)}, j_l^{(1)}], \chi_r^{(1)} = x_{j_r^{(1)}}, \chi_l^{(1)} = x_{j_l^{(1)}}, \chi_S^{(1)} = \frac{\chi_r^{(1)} + \chi_l^{(1)}}{2}$$

We continue until $j_l^{(k)} < j_r^{(k)}$ or until $|\chi_S^{(k)} - \chi_S^{(k-1)}| < e$, with $e = 10^{-8}$ to be a good tolerance for all examined data.

2. *EDE iterative method or Bisection-EDE or BEDE*

We apply to initial data $\{(x_i, \phi_i), i = 0, \dots, n\}$ EDE method and have the 0^{th} output iff $x_{F2} > x_{F1}$:

$$[j_1^{(0)}, j_2^{(0)}], \chi_{F1}^{(0)} = x_{j_1^{(0)}}, \chi_{F2}^{(0)} = x_{j_2^{(0)}}, \chi_D^{(0)} = \frac{\chi_{F1}^{(0)} + \chi_{F2}^{(0)}}{2}$$

If and only if $j_2^{(0)} > j_1^{(0)}$, then we apply again EDE method for data:

$$\{(x_i, \phi_i), i = j_1^{(0)}, \dots, j_2^{(0)}\}$$

and obtain the 1st output for EDE (iff $\chi_{F_2}^{(2)} > \chi_{F_2}^{(1)}$) method:

$$[j_1^{(1)}, j_2^{(1)}], \chi_{F_1}^{(1)} = x_{j_1^{(1)}}, \chi_{F_2}^{(1)} = x_{j_2^{(1)}}, \chi_D^{(1)} = \frac{\chi_{F_1}^{(1)} + \chi_{F_2}^{(1)}}{2}$$

We can also try to produce output for ESE method for each BEDE iteration, but it is not always working, since $[\chi_{F_1}^{(i)}, \chi_{F_2}^{(i)}]$ does not necessary contain $[x_r, x_l]$. Similarly we can produce output for EDE methods for each BESE iteration but again we are not sure that $[x_r^{(i)}, x_l^{(i)}] \supset [\chi_{F_1}^{(i)}, \chi_{F_2}^{(i)}]$.

2 Experiments and Results

We design small experiments by taking a suitable smooth function of known inflection point p , an interval $[a, b]$ that covers all the possible cases $p \in [a, b]$, $p < a$, $p > b$ and we add a uniform error $\epsilon_i \sim U(-r, r)$ via the process 14.

2.1 Symmetric sigmoid curves

We find the points x_1, x_{99} that give the first 1% and the 99% of sigmoid' s capacity L because those points have economic sense. So our interval $[a, b]$ is always relevant to the interval $[x_1, x_{99}]$.

2.1.1 The Fisher-Pry sigmoid curve with total symmetry

Let' s take the function:

$$f(x) = 5 + 5 \tanh(x - 5) \tag{53}$$

after [15], which has $p = 5$, $L = 10$, $x_1 = 2.7024$, $x_{99} = 7.2976$ and examine it at the interval $[2, 8]$ in order to have data symmetry w.r.t. inflection point. The function is also symmetrical around inflection point, i.e. we have *total symmetry*.

From Corollary 1.1 we compute $x_l = 5.970315941$, $x_r = 4.029684059$, $x_{F_1} = 3.850750196$, $x_{F_2} = 6.149249804$, all inside $[2, 8]$, thus all methods are theoretically applicable. We first take $n = 500$ sub-intervals equal spaced without error just for checking our estimators. The results are presented at Table 1. We observe that $\chi_l = 5.9720$, $\chi_r = 4.0280$, $\chi_{F_1} = 3.8480$, $\chi_{F_2} = 6.1520$ are very close to the theoretically expected values, so we are on the results of Lemma 1.3. The absolutely accuracy from the first apply of all

Table 1: Fisher-Pry sigmoid, $p=5$, total symmetry, $n=500$, no-error

$j_r = 170$	$j_l = 332$	$\chi_r = 4.028$	$\chi_l = 5.972$	$\chi_S = 5.0$
$j_{F1} = 155$	$j_{F2} = 347$	$\chi_{F1} = 3.884$	$\chi_{F2} = 6.1520$	$\chi_D = 5.0$

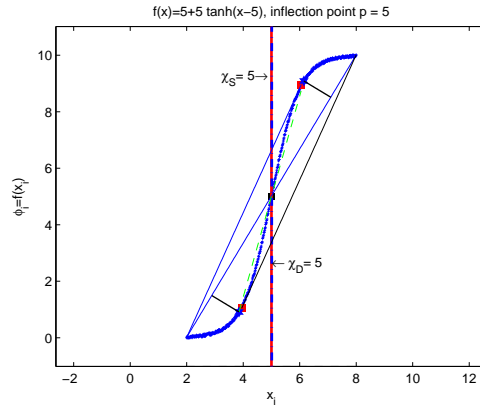


Figure 3: (color online, scaled) Fisher-Pry sigmoid with total symmetry and without error

methods confirms our theoretical analysis. All important lines, curves and points are presented at Figure 3.

We next add the error term $\epsilon_i \sim U(-0.05, 0.05)$ via the process 14 and run our algorithms again. The results are presented at Table 2.

Again the estimations are close to the theoretically expected and both

Table 2: Fisher-Pry sigmoid, $p=5$, data symmetry, $[a, b] = [2, 8]$, $n=500$, error $r=0.05$

$j_r = 163$	$j_l = 339$	$\chi_r = 3.944$	$\chi_l = 6.056$	$\chi_S = 5.000$
$j_{F1} = 155$	$j_{F2} = 349$	$\chi_{F1} = 3.848$	$\chi_{F2} = 6.176$	$\chi_D = 5.012$

methods gave the true answer from the first apply. We present the ESE and EDE intervals and estimators together with the true function and the noisy data at Figure 4, where we present all important points x_l, x_r, x_{F1}, x_{F2} with the relevant tangent lines and the size of the minimum/maximum of F . Due to the *total symmetry* the (dashed) line connecting $(x_{F1}, f(x_{F1})), (x_{F2}, f(x_{F2}))$ passes from the point $(p, f(p))$.

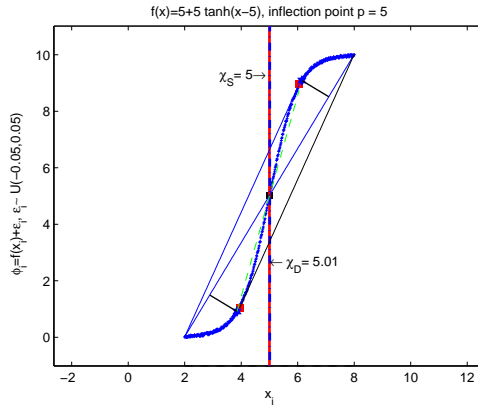


Figure 4: (color online, scaled) Fisher-Pry sigmoid with total symmetry and error $r=0.05$

2.1.2 The Fisher-Pry sigmoid curve with data left asymmetry

We continue with the same sigmoid function, but now we form proper our $[a, b]$ to show data asymmetry w.r.t. inflection point.

Let's take for example [4.2, 8]. If we do our theoretical computations we find $x_l = 5.974322740$, $x_r = 4.029684059$, $x_{F_1} = 4.025677260$, $x_{F_2} = 5.974322740$. We have that $x_r < a$, so χ_r has to estimate $a = 4.2$ and χ_S must be close to 4.703504993. Additionally, $x_{F_1} < a$, so χ_{F_1} must be also an estimation of a , thus χ_D must lie near the value 5.087161370. It's time to see if our theoretical predictions will be confirmed by experiment. We use for comparability the same Standard Partition as before and have the output presented at Table 3. We have confirmation of our theory.

Table 3: Fisher-Pry sigmoid, $p=5$, data left symmetry, $[a, b] = [4.2, 8]$, $n=500$, no error

$j_r = 2$	$j_l = 156$	$\chi_r = 4.2076$	$\chi_l = 5.3780$	$\chi_S = 4.7928$
$j_{F_1} = 1$	$j_{F_2} = 234$	$\chi_{F_1} = 4.2$	$\chi_{F_2} = 5.9708$	$\chi_D = 5.0854$

It is time now to try iterations based on ESE and EDE intervals that contain inflection point and to observe remarkable convergence to the real value of $p = 5$ for both methods. We present ESE & EDE iterations at Table 4.

Table 4: ESE & EDE iterations for Fisher-Pry sigmoid, $p=5$, data left asymmetry, $[a, b] = [4.2, 8]$, $n=500$, no-error

	(a) ESE			(b) EDE		
	χ_r	χ_l	χ_S	χ_{F_1}	χ_{F_2}	χ_D
	4.8156	5.3704	5.0930	4.5192	5.4844	5.0018
	4.8232	5.0892	4.9562	4.7244	5.2716	4.9980
	4.9524	5.0892	5.0208	4.8460	5.1576	5.0018
	4.9600	5.0208	4.9904	4.9068	5.0892	4.99800
	4.9904	5.0208	5.0056	4.9448	5.0512	4.99800

Let's add the same error term $\epsilon_i \sim U(-0.05, 0.05)$ and run our algorithms. The results at Table 5 clearly are close enough to the theoretical expectations.

We observe that ESE method did not estimate the inflection point with acceptable accuracy, so it is time to run the ESE and EDE iterations. The results, Table 6 show a clear improvement of both estimations.

All the points of interesting are presented at Figure 5, where we see that interval does not contain both x_l, x_r and x_{F_1}, x_{F_2} .

Table 5: Fisher-Pry sigmoid, $p=5$, data left symmetry, $[a, b] = [4.2, 8]$, $n=500$, error $r=0.05$

$j_r = 3$	$j_l = 149$	$\chi_r = 4.2304$	$\chi_l = 5.3248$	$\chi_S = 4.7700$
$j_{F1} = 3$	$j_{F2} = 231$	$\chi_{F1} = 4.2152$	$\chi_{F2} = 5.9480$	$\chi_D = 5.0816$

Table 6: ESE & EDE iterations for Fisher-Pry sigmoid, $p=5$, data left asymmetry, $[a, b] = [4.2, 8]$, $n=500$, error $r=0.05$

(a) ESE			(b) EDE		
χ_r	χ_l	χ_S	χ_{F1}	χ_{F2}	χ_D
4.8156	5.3248	5.0702	4.5268	5.5148	5.0208
4.9144	5.1576	5.0360	4.7244	5.2412	4.9828

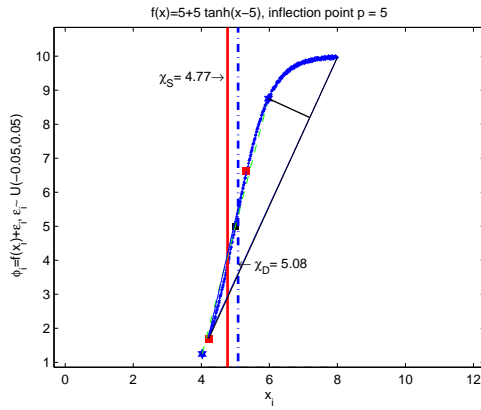


Figure 5: (color online, scaled) Fisher-Pry sigmoid with data left asymmetry and error $r=0.05$

2.2 Non symmetric sigmoid curves

We continue our study with non symmetric sigmoid curves that appear in Economics and other disciplines.

2.2.1 The Gompertz sigmoid curve

Let's examine the function:

$$f(x) = 10 e^{-e^5 e^{-x}} \quad (54)$$

after [16], in the interval [3.5, 8]. The basic properties are presented at Table 7.

It is easy to prove that f is (0.224, 1.0)-asymptotically symmetric around

Table 7: Basic properties of a Gompertz sigmoid

$L = 10$	$x_1 = 3.472820374$	$x_{99} = 9.600149227$
$x_r = 4.138928270$	$x_l = 5.887451706$	$x_S = 5.013189988$
$x_{F1} = 4.095750735$	$x_{F2} = 6.290768183$	$x_D = 5.193259460$

inflection point, so we can handle it similar to a symmetric sigmoid only for a distance of ± 1 from $p = 5$.

We use, for comparison reasons, the same SP with 500 sub-intervals without error and obtain the Table 8 which is absolutely compatible with theoretical predictions. The ESE & EDE iterations are showed at Table 9 where we observe convergence to the real p for both two methods.

Table 8: Gompertz sigmoid, $p=5$, asymmetry, $n=500$, no-error

$j_r = 72$	$j_l = 266$	$\chi_r = 4.139$	$\chi_l = 5.885$	$\chi_S = 5.012$
$j_{F1} = 67$	$j_{F2} = 311$	$\chi_{F1} = 4.094$	$\chi_{F2} = 6.290$	$\chi_D = 5.192$

We can watch the iteration convergence of the two methods in the non error case to the actual value of inflection point at Figure 6 and Figure 7, where we have left the methods to stop when the minimum required points are reached.

We continue with our familiar SP by adding error uniformly distributed by $U(-0.05, 0.05)$ and the results are given at Table 10 while ESE & EDE iterations are shown at Table 11. From these Tables we conclude that convergence to the true value of inflection point $p = 5$ occurs from the iterative

Table 9: ESE & EDE iterations for Gompertz sigmoid, $p=5$, asymmetry, $[a, b] = [3.5, 8]$, $n=500$, no error

(a) ESE			(b) EDE		
χ_r	χ_l	χ_S	χ_{F1}	χ_{F2}	χ_D
4.625	5.489	5.0570	4.4540	5.6690	5.0615
4.778	5.201	4.9895	4.6700	5.3630	5.0165
4.904	5.120	5.0120	4.8050	5.2100	5.0075
4.940	5.048	4.9940	4.8860	5.1200	5.0030
4.976	5.030	5.0030	4.9310	5.0660	4.9985
4.985	5.012	4.9985	4.9580	5.0390	4.9985

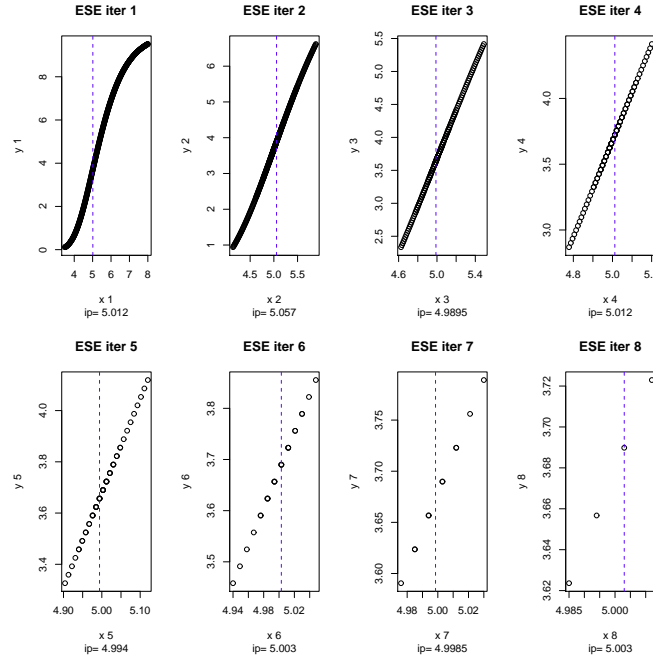


Figure 6: ESE iterations Gompertz asymmetrical sigmoid no error

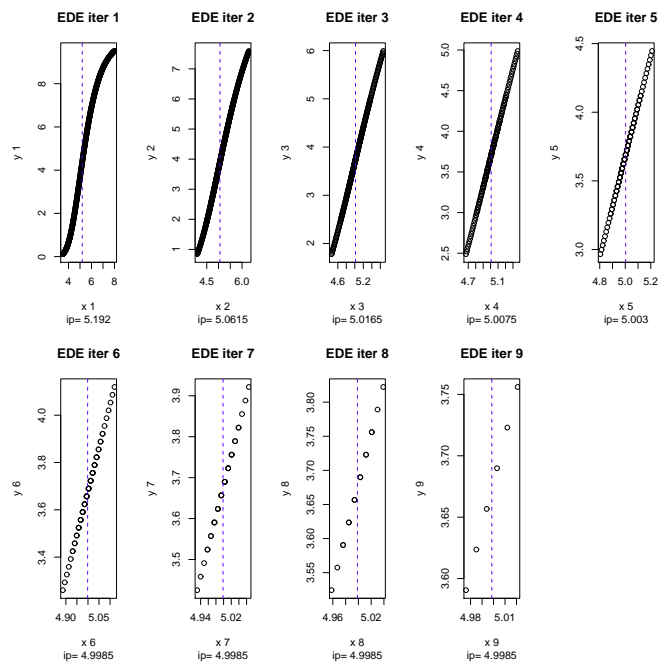


Figure 7: EDE iterations Gompertz asymmetrical sigmoid no error

application of ESE and EDE methods in one or two steps only. All points of interest and data are presented at Figure 8.

Table 10: Gompertz sigmoid, $p=5$, asymmetry, $[a, b] = [3.5, 8]$, $n=500$, error $r=0.05$

$j_r = 74$	$j_l = 274$	$\chi_r = 4.1570$	$\chi_l = 5.9570$	$\chi_S = 5.0570$
$j_{F1} = 66$	$j_{F2} = 319$	$\chi_{F1} = 4.0850$	$\chi_{F2} = 6.3620$	$\chi_D = 5.2235$

Table 11: ESE & EDE iterations for Gompertz sigmoid, $p=5$, asymmetry, $[a, b] = [3.5, 8]$, $n=500$, error $r=0.05$

(a) ESE			(b) EDE		
χ_r	χ_l	χ_S	χ_{F1}	χ_{F2}	χ_D
4.6340	5.5340	5.0840	4.472	5.642	5.057
4.8590	5.1560	5.0075			

2.3 Non sigmoid curves

Our analysis is applicable also to non sigmoid curves, not necessary symmetric or with data symmetry. We shall proceed by making two experiments for a symmetric 3^{rd} order polynomial.

2.3.1 A symmetric 3^{rd} order polynomial with total symmetry

Let the polynomial function:

$$f(x) = -\frac{1}{3}x^3 + \frac{5}{2}x^2 - 4x + \frac{1}{2} \quad (55)$$

We study it at $[-2, 7]$, it has inflection point at $p = 2.5$ and we have *total symmetry* while the interesting points are presented at Table 12.

The SP with 500 sub-intervals without error gives Table 13 which is absolutely compatible with theoretical predictions. There is no need for any kind of iteration, because both methods agree with the true value.

The same SP with uniform error distributed by $U(-2, 2)$ gives the results of Table 14 and two ESE iterations are presented at Table 15. All points and data are shown at Figure 9.

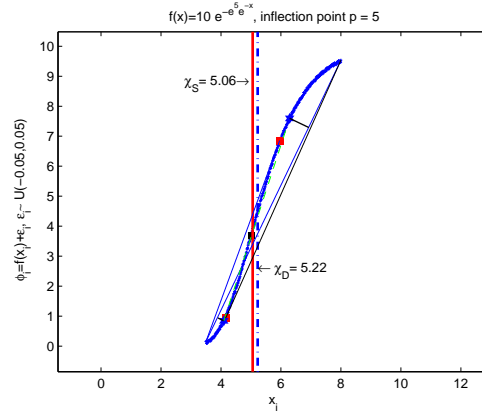


Figure 8: (color online, scaled) Gompertz asymmetrical sigmoid with error $r=0.05$

Table 12: Basic properties of a 3^{rd} order polynomial with total symmetry

$x_r = 0.25$	$x_l = 4.75$	$x_S = 2.50$
$x_{F1} = -0.09807621078$	$x_{F2} = 5.098076211$	$x_D = 2.50$

Table 13: 3^{rd} order polynomial, total symmetry, $p=2.5$, $n=500$, no-error

$j_r = 126$	$j_l = 376$	$\chi_r = 0.25$	$\chi_l = 4.75$	$\chi_S = 2.50$
$j_{F1} = 107$	$j_{F2} = 395$	$\chi_{F1} = -0.092$	$\chi_{F2} = 5.092$	$\chi_D = 2.50$

Table 14: Symmetric 3^{rd} order polynomial, total symmetry, $p=2.5$, $n=500$, error $r=2.0$

$j_r = 115$	$j_l = 375$	$\chi_r = 0.052$	$\chi_l = 4.732$	$\chi_S = 2.392$
$j_{F1} = 105$	$j_{F2} = 375$	$\chi_{F1} = -0.128$	$\chi_{F2} = 4.732$	$\chi_D = 2.302$

Table 15: ESE iterations for 3^{rd} order polynomial, $p=2.5$, total symmetry, $n=500$, error $r=2.0$

χ_r	χ_l	χ_S
1.222	3.688	2.455
1.564	3.382	2.473

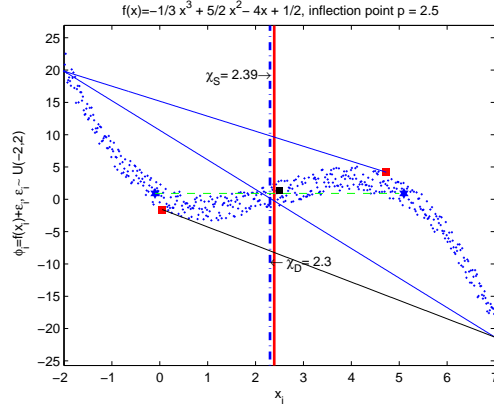


Figure 9: (color online, unscaled) Symmetric 3^{rd} order polynomial with error $r=2.0$

2.3.2 A symmetric 3^{rd} order polynomial with data right asymmetry

For the same symmetric 3^{rd} order polynomial 55 we change the interval to $[-2, 8]$, thus we have data right asymmetry now. Our critical points are written here at Table 16.

Table 16: Basic properties of a 3^{rd} order polynomial with data right asymmetry

$x_r = -0.25$	$x_l = 4.75$	$x_S = 2.25$
$x_{F1} = -0.429732639$	$x_{F2} = 5.429732639$	$x_D = 2.50$

The case of SP with 500 sub-intervals and no error gives Table 17, while ESE and EDE iterations are presented at Table 18. First results are absolutely compatible with theoretical predictions for ESE method.

Table 17: Symmetric 3^{rd} order polynomial, data right asymmetry, $p=2.5$, $n=500$, $[-2, 8]$, no-error

$j_r = 89$	$j_l = 338$	$\chi_r = -0.24$	$\chi_l = 4.74$	$\chi_S = 2.25$
$j_{F1} = 80$	$j_{F2} = 372$	$\chi_{F1} = -0.42$	$\chi_{F2} = 5.42$	$\chi_D = 2.50$

We add uniform error distributed by $U(-2, 2)$ and we have the results

Table 18: ESE & EDE iterations for 3^{rd} order polynomial, $p=5$, $p=2.5$, $n=500$, $[-2, 8]$, no-error

(a) ESE			(b) EDE		
χ_r	χ_l	χ_S	χ_{F1}	χ_{F2}	χ_D
1.3800	3.8800	2.6300	0.82000	4.1800	2.5000
1.8000	3.0600	2.4300			
2.2200	2.8600	2.5400			
2.3200	2.6400	2.4800			
2.4200	2.5800	2.5000			
2.4600	2.5400	2.5000			

of Table 19, while one ESE & one EDE iteration are given at Table 20. All points and data are presented at Figure 10.

Table 19: Symmetric 3^{rd} order polynomial, data right asymmetry, $p=2.5$, $n=500$, $[-2, 8]$, error $r=2.0$

$j_r = 88$	$j_l = 338$	$\chi_r = -0.26$	$\chi_l = 4.74$	$\chi_S = 2.24$
$j_{F1} = 88$	$j_{F2} = 384$	$\chi_{F1} = -0.26$	$\chi_{F2} = 5.66$	$\chi_D = 2.70$

Table 20: ESE & EDE iterations for 3^{rd} order polynomial, $p=2.5$, $n=500$, $[-2, 8]$, error $r=2.0$

(a) ESE			(b) EDE		
χ_r	χ_l	χ_S	χ_{F1}	χ_{F2}	χ_D
1.46	3.84	2.65	0.86	3.84	2.35

There exist a problem here. Although we have a symmetric polynomial, the TESE is not equal to the true inflection point. A remedy for this problem for the class of 3^{rd} order polynomials is given with the next Lemma.

Lemma 2.1 *The 3^{rd} order polynomial ESE correction.*

Let a 3^{rd} order polynomial $f(x) = \alpha x^3 + \beta x^2 + \gamma x + \delta$ and let p its inflection point. Then it holds exactly that:

$$p = \frac{1}{3}x_l + \frac{1}{3}x_r + \frac{1}{6}a + \frac{1}{3}b \quad (56)$$

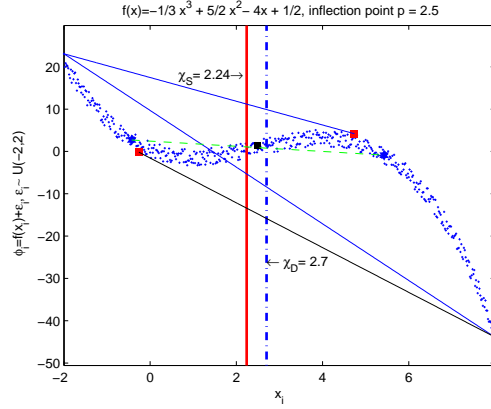


Figure 10: (color online, unscaled) Symmetric 3rd order polynomial with data right asymmetry

and

$$\hat{p} = \frac{1}{3} \chi_l + \frac{1}{3} \chi_r + \frac{1}{6} a + \frac{1}{3} b$$

is a consistent estimator of trapezoidal estimated p .

Proof

The inflection point because $\alpha \neq 0$ is found from the root of the second derivative, i.e. $6\alpha p + 2\beta = 0$ or $p = -\frac{\beta}{3\alpha}$. Due to Corollary 1.1 we have for the x_l that:

$$3\alpha x^2 + 2\beta x + \gamma = \frac{\alpha x^3 + \beta x^2 + \gamma x - \alpha a^3 - \beta a^2 - \gamma a}{x - a}$$

or

$$(x - a)^2 (\alpha a + \beta + 2\alpha x) = 0$$

so the internal solution x_l is:

$$x_l = -\frac{\alpha a + \beta}{2\alpha} \tag{57}$$

For the x_r we have similar that:

$$3\alpha x^2 + 2\beta x + \gamma = \frac{\alpha b^3 + \beta b^2 + \gamma b - \alpha x^3 - \beta x^2 - \gamma x}{b - x}$$

or

$$(b - x)^2 (\alpha b + \beta + 2\alpha x) = 0$$

so the internal solution x_r is:

$$x_r = -\frac{\alpha b + \beta}{2\alpha} \quad (58)$$

By adding x_l and x_r we obtain:

$$x_l + x_r = -\frac{1}{2}a - \frac{\beta}{\alpha} - \frac{1}{2}b$$

and if we remember that $p = -\frac{\beta}{3\alpha}$ we obtain:

$$x_l + x_r = -\frac{1}{2}a + 3p - \frac{1}{2}b$$

or finally

$$p = \frac{1}{3}x_l + \frac{1}{3}x_r + \frac{1}{6}a + \frac{1}{3}b \quad (59)$$

Since we have proven that χ_l, χ_r are consistent estimators of trapezoidal calculated values of x_l, x_r we can take a consistent estimation for trapezoidal calculated p by replacing the unknown x_l, x_r with the estimators χ_l, χ_r . \square

As an example, we come back to the case of 3^{rd} order symmetric polynomial with data right asymmetry. We have that $a = -2, b = 8$ and from Table 19 is $\chi_r = -0.26, \chi_l = 4.74$, so we have that:

$$\hat{p} = \frac{1}{3}\chi_l + \frac{1}{3}\chi_r + \frac{1}{6}a + \frac{1}{3}b = 2.493333333$$

which is much closer to the true value of 2.5.

The above analysis can be extended to every function, if we can find analytically a relation between inflection point and x_l, x_r, a, b .

3 Discussion

The sigmoid or S-shaped pattern is common in many disciplines: utility theory [1] & technological substitution models [2, 3] in Economics, growth theory [4] & allosterism [5] in Biology, population dynamics [6, 7] in Ecology, titration data analysis [8] & autocatalysis [9] in Analytical Chemistry, dose-response [10] in Medicine and many others. Starting from the problem of identifying the inflection point for the data $\{(x_i, \phi_i), i = 0, 1, \dots, n\}$ we have created two geometrical methods in order to solve this problem: the

Extremum Surface Estimator (ESE method) and the Extremum Distance Estimator (EDE method). We did not perform neither regression nor splines representation analysis. In addition, no concepts like discrete or digital curvature were defined or used. Instead we focused on finding two points where the true inflection point lies between and then we took as estimator the middle point, just like in bisection method.

The methods can be applied iteratively similarly to bisection method and converge to the true inflection point either from the first or after a few iterations only. The R Package *inflection* is available at [17] for using ESE & EDE methods with R. Other implementations for the methods have been done with FORTRAN, Maple and Matlab. If we have large data sets then FORTRAN is more efficient, for example the problem of estimating the inflection point of $n = 10000$ data pairs needed less than 7 sec CPU time in FORTRAN GNU compiler and a typical Intel Core i5 CPU with 4 GB RAM memory.

References

- [1] M. Friedman and L.J. Savage, The Utility Analysis of Choices Involving Risk, *Journal of Political Economy*, Vol. **56**, No. 4, pp. 279-304, (1948).
- [2] C. Marchetti and N. Nakicenovic, The Dynamics of Energy Systems and the Logistic Substitution Model, *International Institute for Applied Systems Analysis*, RR-**79-13**, Laxenburg, Austria, (1979).
- [3] T. Modis, Predictions, *Simon and Schuster*, New York, (1992)
- [4] L. von Bertalanffy, Principles and theory of growth, in *Fundamental Aspects of Normal and Malignant Growth*, W. W. Nowinski (ed), New York: Elsevier, pp. 137-259, (1960).
- [5] W. Bardsley and R. Childs, Sigmoid Curves, Nonlinear Double-Reciprocal Plots and Allosterism, *Biochemical Journal*, **149**, pp. 313-328, (1975).
- [6] P.F. Verhulst, Notice sur la loi que la population suit dans son accroissement, *Correspondance Mathimatique et Physique*, **10**,113-121, (1838).
- [7] P. Turchin, *Complex Population Dynamics: A Theoretical/Empirical Synthesis*, Princeton University Press, (2003).

- [8] F. Mohr, *Lehrbuch der chemisch-analytischen Titrimethode: Nach eigenen versuchen. (Textbook of analytical-chemical titration methods)*, Braunschweig: Freidrich Vieweg und Sohn, (1877).
- [9] S.K. Upadhyay, *Chemical Kinetics and Reaction Dynamics*, Springer, (2006).
- [10] J.B. Meddings and R.B. Scott and G.H. Fick, Analysis and comparison of sigmoidal curves: application to dose-response data, *Am J Physiol Gastrointest Liver Physiol* December 1, **257**:(6) G982-G989, (1989).
- [11] J. H. Han and T. Poston, Chord-to-point distance accumulation and planar curvature: a new approach to discrete curvature, in *Pattern Recognition Letters*, **22**, pp 1133 - 1144, (2001).
- [12] M. Mokji and S.A.R. Abu Bakar Starfruit shape defect estimation based on concave and convex area of a closed planar curve, in *Jurnal Teknologi*, **48** (D), pp. 7589, (2008).
- [13] Sven Loncaric, A survey of shape analysis techniques, in *Pattern Recognition*, Volume **31**, Issue 8, Pages 983-1001, (1998).
- [14] F. Mokhtarian and A. Mackworth, Scale-based description and recognition of planar curves and two-dimensional shapes, in *IEEE Transactions on Pattern Analysis and Machine Intelligence*, **8**(1), pp 3443, (1986).
- [15] J.C. Fisher and R.H. Pry, A Simple Substitution Model of Technological Change, *Technological Forecasting and Social Change*, **3**, pp. 5-88, (1971).
- [16] B. Gompertz, On the Nature of the Function Expressive of the Law of Human Mortality, and on a New Mode of Determining the Value of Life Contingencies, *Philosophical Transactions of the Royal Society of London*, **115**, pp. 513-585, (1825).
- [17] D.T. Christopoulos, *inflection: Finds the inflection point of a curve.*, R package version 1.1.; software available at <http://CRAN.R-project.org/package=inflection>, (2013).